https://doi.org/10.5194/egusphere-2025-1848
Preprint. Discussion started: 12 June 2025

An extrapolation algorithm for estimating river bed grain size distributions across basins

Jordan T. Gilbert[1,2]

[1]Department of Geosciences, University of Montana, Missoula, MT 59812-1296, United States

[2]Department of Watershed Sciences, Utah State University, Logan, UT 84322, United States

Correspondence to: Jordan Gilbert (jordan.gilbert@usu.edu)

Abstract. Values representing grain size distributions of stream reaches are essential for estimating sediment transport at the reach scale. Various modeling frameworks exist that attempt to simulate reach-scale sediment transport across entire drainage basins to characterize sediment dynamics at a watershed scale. Such frameworks require estimates of grain size at each reach. Because obtaining direct measurements at this scale is impractical and logistically difficult, methods to estimate or extrapolate grain size measurements are needed, however, few currently exist. Here I present an extrapolation algorithm that uses one or more pebble counts to extrapolate full grain size distributions to each reach of a drainage network. In addition to the pebble count measurements, the tool requires a stream network geospatial feature class, attributed with values for reach-averaged slope and some consistent measure of relative flow magnitude (or a proxy for flow). I tested the tool in a set of sub-watersheds in the Bitterroot River basin of western Montana, US, with varying valley morphologies, and compared predictions to measurements at 16 sites. When using multiple measurements for calibration, prediction errors averaged 5.8% of the measured grain sizes. When using a single measurement for calibration, errors averaged 8.4%.

1 Introduction

A characterization of the bed surface grain size distribution (GSD) of rivers is essential for applying sediment transport formulae to estimate transport rates and total yield. In cases where the bed can be assumed to be equally mobile, a single characteristic size (e.g. median grain size, D_{50}) is often used to represent the bed material (e.g.,

https://doi.org/10.5194/egusphere-2025-1848
Preprint. Discussion started: 12 June 2025

Meyer-Peter & Müller, 1948). In contrast, to apply fractional transport equations (e.g., Parker, 1990; Wilcock & Crowe, 2003), a GSD is needed. GSD data can be tedious and time consuming to collect, however, and spatial coverage within a given area can be limited by accessibility to channels. Application is, therefore, generally limited in spatial extent unless GSDs can be estimated for locations without direct measurements.

Two general methods are typically used for quantifying GSDs: pebble counts and photo sieving. Pebble counts (often referred to as Wolman pebble counts after Wolman (1954)) are a simple method of characterizing bed GSDs by randomly gathering particles from the bed surface within a defined extent, and measuring the b-axis diameter of each. Sampling bias is common as larger particles are easier to see and are typically touched first as they protrude from the bed more, especially in poorly sorted mixtures (Leopold, 1970; Wohl et al., 1996). To avoid sampling bias, protocols have been recommended when performing pebble counts. For example, a "random walk" method is often used, with the sampler moving randomly across the defined area, identifying the particle at the point of the foot at each step and *then* retrieving it, rather than reaching down and grabbing the first particle touched. Kondolf (1997) recommends performing individual pebble counts for unique populations (geomorphic units) within a reach and taking the area-weighted average to characterize the whole reach. Another method uses a grid system, identifying the particle directly beneath each intersection and retrieving it as part of the count (Bunte & Abt, 2001). Typical pebble counts consist of 100 particles; fewer may be needed to characterize relatively homogenous beds, and more may be needed in poorly sorted beds with a wide GSD. Additionally, multiple pebble counts can be performed for a given location by a single person or multiple individuals, and the results used to quantify uncertainty in the values used (e.g., D_{50}). Despite the drawbacks of this method related to sampling bias, it is easy to implement, provides good characterizations of river beds, and is the most widely used method.

Photo sieving is a methodology in which image processing algorithms are used to identify individual grains in photographs and calculate their diameter (Ibbeken & Schleyer, 1986). The advantages of this method are that rather than a random sample, all identifiable particles can be used to generate the GSD, and it can be applied over large areas wherever photographs are available. These algorithms have been improved upon with advances in computer vision technology (e.g., Buscombe, 2008), including even broader application with the advent of drone-based

https://doi.org/10.5194/egusphere-2025-1848
Preprint. Discussion started: 12 June 2025

surveys, which can produce orthoimagery of very large areas of river bed (e.g., Purinton & Bookhagen, 2019). Drawbacks of this method are that it can only be effectively applied where grains are exposed and easily identifiable in images, and that partially buried or obscured grains that are still part of the surface layer cannot be accurately measured. This methodology, therefore, cannot be applied to inundated or densely vegetated areas. Where applicable, photo sieving produces results comparable to pebble counts (Strom et al., 2010). Where it is appropriate to use, photo sieving can characterize grain size over larger spatial scales than pebble counts, however, like pebble counts, it is an impractical method for quantifying GSDs across entire drainage networks.

Controls on grain size include various factors relating to sediment production processes, as well as hydraulic sorting of bed material. For example, lighology exerts control on sediment delivery rates to channels, as well as the size of that sediment (Mueller et al., 2016). The size of individual grain produced from a rock layer is also a function o fracture spacing within the rock (Neely & DiBiase, 2020; Vericat et al., 2021). When sediment is delivered to channels from hillslope erosion processes, hydraulic sorting then exerts control on what sizes are present in the bed at a given reach (Snelder et al., 2011). As a result, variables often associated with sediment transport (i.e., channel gradient and flow magnitude) also correlate with bed GSD (Cohen et al., 2022).

Various sediment models seek to simulate transport across drainage networks in a spatially explicit manner (e.g., Czuba, 2018; Gilbert & Wilcox, 2020; Schmitt et al., 2016), and thus require a specification of grain size at each spatially distinct location in the modeling domain. These models have traditionally used relatively simple approaches, including applying the same distribution to the entire network, or correlating a median grain size with topographic and hydrologic information. A systematic method for estimating full distributions across drainage networks would thus be a valuable contribution for improving existing sediment transport and connectivity models.

Several approaches have been used to estimate grain size across large spatial extents. Jha et al. (2022) assessed D_{50} at over 2,400 locations from five different sources and used inverse distance weighted interpolation to estimate D_{50} regionally between sample points. This provides broad regional patterns, but does not provide information in

https://doi.org/10.5194/egusphere-2025-1848
Preprint. Discussion started: 12 June 2025

specific catchments or reaches. Abeshu et al. (2022) attributed D_{50} information from 2,577 United States Geologic Survey (USGS) gages to corresponding reaches in the National Hydrography Dataset (NHD) and used machine learning to develop a model based on the attributes available in the in NHDPlus dataset, finding that slope and distance between the reach and the streams mouth were the most important channel characteristic predictors of grain size. Similarly, Snelder etl a. (2011) used random forest models to assess data from 677 stream reaches in France with grain size measurements and found that the model incorporating variables related to hydraulic sorting (e.g., slope and precipitation) best predicted D_{50}.

Other approaches for estimating grain size across large spatial scales have used remote sensing-based methods. For example, Snyder et al. (2013) used digital elevation models to predict grain size. Their approach requires spatially distributed estimates of Manning's n roughness values, and is based upon the assumption that critical Shields stress (τ^*_c) is 0.04 and that it is approximately equal to the Shields stress of a 2-year recurrence-interval flood. Similarly, models based on Shields stress (Buffington et al., 2004) and stream power (Gorman et al., 2011), calibrated empirically with both GIS and field data, have been used to develop predictive grain size models. However, all of the approaches described here estimate only the D_{50}, and no method currently exists that predicts full GSDs across drainage networks, despite the fact that such information would be useful for a variety of purposes.

In this paper, I introduce a method for extrapolating grain size distributions throughout a drainage network based on one or more measurements (e.g., obtained using pebble counts or photo sieving). This method, similar to previous approaches, has the advantage of being calibrated based on actual measurements for a basin, while utilizing remote sensing data to obtain topographic data. It also predicts a full grain size distribution for each reach, rather than just D_{50}, allowing for application of fractional sediment transport functions. Because hillslope sediment delivery is one control on grain sizes present within a reach (Hassan et al., 2019), this approach is best suited to fully alluvial river systems, or systems where the magnitude of hillslope sediment production is not highly spatially variable.

https://doi.org/10.5194/egusphere-2025-1848
Preprint. Discussion started: 12 June 2025

2 Methods

The grain size tool presented here can use a single measurement, or multiple measurements of GSD to extrapolate estimates of D_{16} (the particle size for which 16% of the bed is finer), D_{50}, and D_{84} (the particle size for which 84% of the bed is finer), along with an uncertainty range for each to every segment or reach of a geospatial drainage network layer. The tool then generates an estimate of full GSDs for each reach (i.e., the fraction of each half-phi size class in the bed; this information is stored in a '.json' file). The tool requires an input drainage network GIS feature class, for which GSDs will be estimated and attributed to each feature. The layer should include attributes representing reach-averaged slope and some measure of flow or a proxy for flow magnitude (e.g., a two-year recurrence interval flow or drainage area; I used cumulative annual precipitation within the basin upstream of each reach), with a value for each feature.

2.1 Algorithm

Two different processes can be used, depending on whether one or multiple pebble count measurements are being used for calibration. For best results, multiple measurements spanning a range of stream sizes and gradients should be used. However, data availability is often limited, sometimes to a single measurement for a basin, so the tool also uses a novel algorithm to estimate GSDs in such circumstances. The algorithm steps are listed below, followed by more in-depth descriptions.

Both (single measurement and multiple measurements):

1) Calculate D_{16}, D_{50}, and D_{84} and their uncertainty for measurement reach(es) from GSD measurements (pebble counts).

Single Measurement:

2) Find the flow depth required to transport the D_{16}, D_{50}, and D_{84} at the measurement reach (critical depth).

3) Find hydraulic geometry coefficients associated with the critical depth.

https://doi.org/10.5194/egusphere-2025-1848
Preprint. Discussion started: 12 June 2025

4) Extrapolate critical depth to each drainage network segment based on a parameterized hydraulic geometry relationship.

5) Estimate D_{16}, D_{50}, and D_{84} at each segment using the Shields equation and a chosen method for estimating critical Shields stress.

Multiple:

6) Calibrate functions for D_{16}, D_{50}, and D_{84} that relate grain sizes to the product of slope and flow using all available measurements.

7) Estimate D_{16}, D_{50}, and D_{84} at each segment using calibrated empirical function.

Both:

8) Fit skew-normal distribution parameters (location, scale, and shape) for each pebble count measurement. Take the average value of each parameter to use as a starting point in estimating the parameters for non-measurement reaches.

9) For each drainage network segment, fit new skew-normal distribution parameters using the parameters from the measurement reaches as a starting point. These parameters are adjusted until the error between D_{16}, D_{50}, and D_{84} found from generating a new distribution is minimized compared against the actual values attributed to the segment in step 5 or 7.

10) Generate a distribution using the solved parameters, removing fractions finer than sand for the segment. Calculate the fraction of the resulting distribution within each half-phi size interval and store the data in the output .json file.

2.1.1 Calculating D_{16}, D_{50}, and D_{84} from measurements and quantifying uncertainty

For each pebble count, the data is bootstrapped with replacement 100 times and sampled until the number of values is 80% of the total number of measurement values. For each bootstrap, the 16^{th}, 50^{th}, and 84^{th} percentile of the data is recorded, generating a distribution of each consisting of 100 values. The values for D_{16}, D_{50}, and D_{84} are then set

https://doi.org/10.5194/egusphere-2025-1848
Preprint. Discussion started: 12 June 2025

as the mean of these distributions with the uncertainty being characterized as plus or minus two standard deviations. Additionally, the reach slope and flow attribute are recorded (from the drainage network attributes) in order to parameterize relationships between the product of slope and flow and the different grain sizes.

2.1.2 Critical Depth

In the case where a pebble count at a single location is used, after the D_{16}, D_{50}, and D_{84} are calculated, the depth required to mobilize each of these sizes (critical depth) is estimated using the Gilbert and Wilcox (2024a) method for calculating critical Shields stress, along with the Shields function. Critical Shields stress for a given grain size D_i is calculated as

$$\tau^*_{c,i} = a\left(\frac{D_i}{D_{50}}\right)^{-0.67} \quad (1)$$

where the subscript *i* denotes a given grain size fraction, and the coefficient *a* varies as a function of the D_{84} to D_{50} ratio,

$$a = 0.029 \; if \; \frac{D_{84}}{D_{50}} \leq 2 \quad (2a)$$

$$a = 0.043 ln\left(\frac{D_{84}}{D_{50}}\right) - 0.0005 \; if \; \frac{D_{84}}{D_{50}} > 2 \quad (2b)$$

The critical Shields number is given by the function

$$\tau^*_{c,i} = \frac{\tau_{c,i}}{(\rho_s - \rho)gD} \quad (3)$$

https://doi.org/10.5194/egusphere-2025-1848
Preprint. Discussion started: 12 June 2025

where $\tau_{c,i}$ is the critical boundary shear stress at which the i^{th} size fraction of the bed becomes mobile. Shear stress is typically estimated using the depth-slope product (which assumes steady, uniform flow),

$$\tau = \rho g h S. \quad (4)$$

In equations 3 and 4, g is acceleration due to gravity (9.81 m/s^2), ρ_s is the density of sediment (2650 kg/m^3), ρ the density of water (1000 kg/m^3), h is average flow depth (m), and S is reach averaged slope (m/m). τ can be solved for by multiplying the denominator of the Shields function by τ^*, and critical depth for the size fraction i can then be estimated by rearranging the depth-slope product,

$$h_{c,i} = \frac{\tau_{c,i}}{\rho g S}. \quad (5)$$

2.1.3 Hydraulic Geometry Coefficients

In order to extrapolate critical depth values to each drainage network segment, hydraulic geometry coefficients are parameterized. Hydraulic geometry equations scale channel geometry with discharge (Leopold & Maddock, 1953). In downstream hydraulic geometry relationships, an exponent of 0.4 is often used for depth (Morel et al., 2020):

$$h = \alpha Q^{0.4} \quad (6)$$

where Q is discharge. In this case, Q can be substituted for drainage area *or* whatever other flow proxy attribute is being used. α is simply solved for in the measurement reach, and used for every other drainage network segment.

https://doi.org/10.5194/egusphere-2025-1848
Preprint. Discussion started: 12 June 2025

2.1.4 Estimating Grain Size (Single Measurement)

After the coefficient in equation 6 is calculated, critical depth for D_{16}, D_{50}, and D_{84} is estimated for each reach, based on the reach's flow proxy attribute value. Shear stress at that depth is calculated using equation 4 with the calculated critical depth, and then the Shields formula (equation 3) is rearranged to solve for *D*.

$$D_i = \frac{\tau_{c,i}}{(\rho_s - \rho) g \tau_{c,i^*}} \quad (7)$$

where the subscript *i* represents the specific grain size percentile (i.e., 16, 50, 84).

2.1.5 Estimating Grain Size (Multiple Measurements)

When multiple pebble counts are used with the tool, three functions are parameterized to calculate D_{16}, D_{50}, and D_{84} respectively. For each of the three grain size fractions, a least squares regression is used to fit a relationship predicting grain size as a function of the product of slope and flow (Figure 1). The interaction of these two variables is largely able to explain variation in grain size. When reaches are steeper, they tend to have coarser beds, as flow competence is higher and larger particles can be mobilized. However, a steep headwater stream with little flow will have a much finer GSD than a higher-order stream with the same slope, where the combination of slope and flow result in much greater flow competence. The values of slope and flow for every other reach in the drainage network are then used to predict D_{16}, D_{50}, and D_{84} using the fitted relationships.

https://doi.org/10.5194/egusphere-2025-1848
Preprint. Discussion started: 12 June 2025

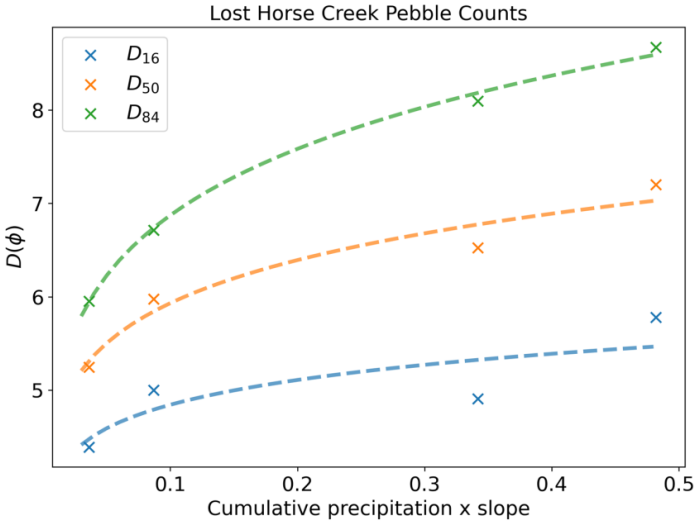

Figure 1. Parameterized relationships (lines) for calculating D_{16}, D_{50}, and D_{84} as a function of the product of slope and flow using four pebble counts within a single basin.

220 **2.1.6 Estimating Full Grain Size Distributions**

For each grain size measurement, the data is converted to phi values. Typically, phi value distributions for coarse-bedded channels are negatively skewed. The parameters of a best-fit skew-normal distribution (location, scale, and shape) are therefore calculated (Figure 2A). In the case of multiple measurements, the parameters are found for each measurement, and the mean value of each parameter is used as a starting point for estimating parameters at each
225 individual reach.

For each network reach, a distribution is generated using the parameters calculated from the measurement data. An optimization process is then implemented, varying the parameters until the errors between D_{16}, D_{50}, and D_{84} of a distribution generated from the new parameters and the values of D_{16}, D_{50}, and D_{84} calculated for that segment
230 previously are minimized (Figure 2B). These optimized parameters are used to generate a final distribution. Values

https://doi.org/10.5194/egusphere-2025-1848
Preprint. Discussion started: 12 June 2025

finer than sand are removed (in this application to coarse bedded rivers). From the remaining values, the fraction within each half-phi size interval is calculated, and the values stored in a .json file.

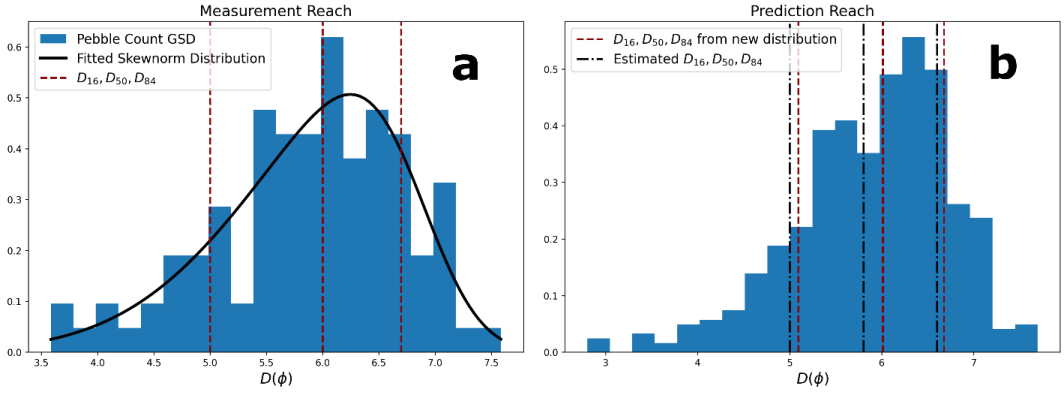

Figure 2. Pebble count measurements are used to fit a skew-normal distribution and calculate its parameters (A). Those parameters are then used to generate new distributions in non-measurement (prediction) reaches (B). The parameters are then adjusted until the errors between D_{16}, D_{50}, and D_{84} from newly generated distributions and previously predicted values for D_{16}, D_{50}, and D_{84} are minimized.

3 Application

To test its effectiveness, I applied the algorithm to two collections of mountain river sub-basins within the larger Bitterroot River basin of Western Montana (Figure 3). Within each basin, I performed pebble counts at several locations spatially dispersed across the watershed, capturing varying stream sizes and gradients. One basin in each collection was used to calibrate the model, after which it was applied to the remaining basins. The first collection consisted of basins with dendritic networks flowing through v-shaped valleys, where steep hillslopes physically connected to channels are prevalent throughout the watersheds (Woods, Rye, Sleeping Child, and Burnt Fork Creeks). The second collection was made up of streams within formerly glaciated mountain basins (Blodgett, Roaring Lion, and Lost Horse Creeks), with u-shaped valleys and wider valley bottoms, and greater variability in gradients of hillslopes adjacent to channels as a result of complex erosion patterns and valley geometries common in

https://doi.org/10.5194/egusphere-2025-1848
Preprint. Discussion started: 12 June 2025

250 post-glacial landscapes (Hassan et al., 2019). Because of the greater uniformity in hillslope gradients adjacent to channels in first group, I infer generally high hillslope-channel connectivity, and refer to this group hereafter as the 'uniform group.' In the second group, because hillslope gradients adjacent to channels were lower and more variable, I infer lower and more variable hillslope-channel connectivity, and refer to this group hereafter as the 'variable group.' After running the model using multiple calibration measurements, I ran it for each basin using a
255 single calibration measurement within the basin, allowing for comparison of results using the two methods.

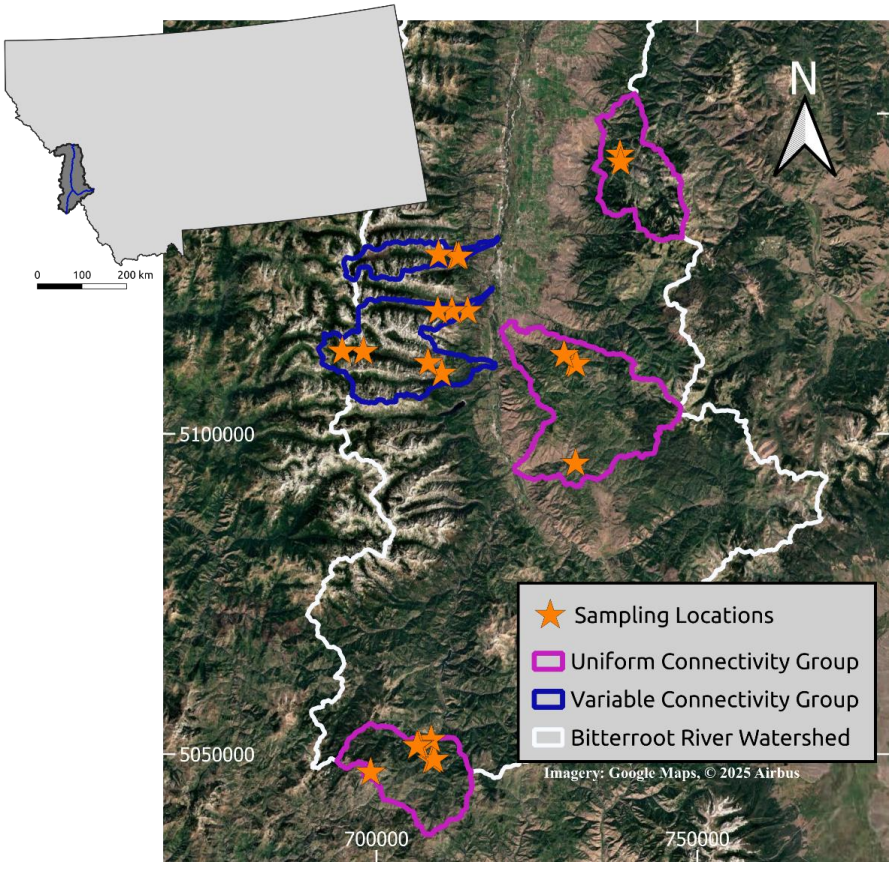

Figure 3. Locations of grain size sampling within the Bitterroot River basin, and the location of the Bitterroot basin within Montana. Coordinates are in WGS84 UTM 11N. Imagery: Google Maps, © 2025 Airbus.

https://doi.org/10.5194/egusphere-2025-1848
Preprint. Discussion started: 12 June 2025

260

4 Results

For model results using multiple pebble count measurements for calibration (Table 1), the average discrepancy between predicted and measured size was 6 mm for D_{16}, 14 mm for D_{50}, and 32 mm for D_{84}. In comparing predictions to measurements in the phi scale, this equates to errors of 7.7% of the measured size for D_{16}, 5.3% for
265 D_{50}, and 4.4% for D_{84}. All combined, the average prediction error was 5.8%. With the exception of D_{84}, which had similar error in both cases, errors were lower for the uniform group (6%, 4.1%, and 5%) than for the variable group (9.1%, 6.4%, and 3.9%).

Within the uniform group, the geology of three of the four watersheds is primarily metamorphic (gneisses and
270 schists). By contrast, the fourth basin is underlain by sedimentary and metasedimentary (e.g., quartzite) rocks. If the two sites with different geology than the others (BF and GC) are excluded, error is further reduced (5.1%, 1.9%, and 2.5%). In the variable group, errors were the highest where GSD was overpredicted in a very low-gradient, unconfined reach.

275 *Table 1. Grain size estimate results using multiple calibration measurements.*

		Measured			*Predicted*			*Difference (mm)*			*Difference (% phi)*		
	Site	**D16**	**D50**	**D84**	**D16**	**D50**	**D84**	**D16**	**D50**	**D84**	**D16**	**D50**	**D84**
Uniform connectivity	**WC1**	15	35	73	12	35	76	3	0	3	8.2%	0.0%	0.9%
	WC2	24	48	87	16	45	103	8	3	16	12.8%	1.7%	3.8%
	WC3	5	15	37	5	15	37	0	0	0	0.0%	0.0%	0.0%
	RC	15	50	128	19	57	142	4	7	14	8.7%	3.3%	2.1%
	SC1	30	88	208	30	87	213	0	1	5	0.0%	0.3%	0.4%
	SC2	35	71	130	30	85	208	5	14	78	4.3%	4.2%	9.7%
	TB	21	53	150	22	62	152	1	9	2	1.5%	4.0%	0.3%
	BF	39	69	120	26	84	205	13	15	85	11.1%	4.6%	11.2%
	GC	14	29	66	17	54	132	3	25	66	7.4%	18.5%	16.5%
	Average							**4**	**8**	**30**	**6.0%**	**4.1%**	**5.0%**
Va	**LHSF**	30	96	291	40	116	291	10	20	0	8.5%	4.1%	0.0%

https://doi.org/10.5194/egusphere-2025-1848
Preprint. Discussion started: 12 June 2025

LHNF	57	150	380	45	137	370	12	13	10	5.8%	1.8%	0.4%
LHO	35	65	104	29	61	115	6	4	11	5.3%	1.5%	2.2%
LHP	21	39	63	22	40	62	1	1	1	1.5%	0.7%	0.4%
RL	32	76	184	33	84	190	1	8	6	0.9%	2.3%	0.6%
RLTX	28	83	286	43	148	436	15	65	150	12.9%	13.1%	7.5%
RLA	11	22	40	25	50	87	14	28	47	34.2%	26.6%	21.1%
BC	38	84	172	33	80	178	5	4	6	3.9%	1.1%	0.7%
BCF	37	97	304	46	138	396	9	41	92	6.0%	7.7%	4.6%
BCG	20	52	137	29	64	129	9	12	8	12.4%	5.3%	1.2%
Average							**8**	**20**	**33**	**9.1%**	**6.4%**	**3.9%**
Average (all)							**6**	**14**	**32**	**7.6%**	**5.3%**	**4.4%**

Using a single calibration measurement (Table 2), errors were slightly higher than they were using multiple calibration measurements (11 mm, 21 mm, 48 mm; 13.1%, 6.6%, 5.7%). The average error of all measurements was 8.4%.

Table 2. Grain size estimate results using single calibration measurements.

		Measured			*Predicted*			*Difference (mm)*			*Difference (% phi)*		
	Site	**D16**	**D50**	**D84**	**D16**	**D50**	**D84**	**D16**	**D50**	**D84**	**D16**	**D50**	**D84**
Variable connectivity	**BC**	38	84	172	37	87	173	1	3	1	0.7%	0.8%	0.1%
	BCF	37	97	304	87	206	452	50	109	148	23.7%	16.5%	6.9%
	BCG	20	52	137	25	60	115	5	8	22	7.4%	3.6%	3.6%
	LHSF	30	96	291	28	88	270	2	8	21	2.0%	1.9%	1.3%
	LHNF	57	150	380	56	174	530	1	24	150	0.4%	3.0%	5.6%
	LHO	35	65	104	12	48	146	23	17	42	30.1%	7.3%	7.3%
	LHP	21	39	63	11	33	101	10	6	38	21.2%	4.6%	11.4%
	RL	32	76	184	29	77	184	3	1	0	2.8%	0.3%	0.0%
	RLTX	28	83	286	70	184	466	42	101	180	27.5%	18.0%	8.6%
	RLA	11	22	40	13	33	77	2	11	37	7.0%	13.1%	17.8%
Uniform connectivity	**WC1**	15	35	73	16	32	53	1	3	20	2.4%	2.5%	7.5%
	WC2	24	48	87	23	46	82	1	2	5	1.3%	1.1%	1.3%
	WC3	5	15	37	13	26	53	8	11	16	59.4%	20.3%	10.0%
	SC1	30	88	208	36	73	130	6	15	78	5.4%	4.2%	8.8%
	SC2	35	71	130	36	74	134	1	3	4	0.8%	1.0%	0.6%

https://doi.org/10.5194/egusphere-2025-1848
Preprint. Discussion started: 12 June 2025

TB	21	53	150	35	71	145	14	18	5	16.8%	7.4%	0.7%
Average (all)							**11**	**21**	**48**	**13.1%**	**6.6%**	**5.7%**

One useful feature of the model is that it attributes geospatial data with the grain size predictions. Figure 4 highlights how this allows for identification of spatial patterns in grain size throughout a basin. As qualitative validation of these spatial patterns, obvious differences in grain size distributions of different reaches based on photographs are captured in the model predictions (Figure 5).

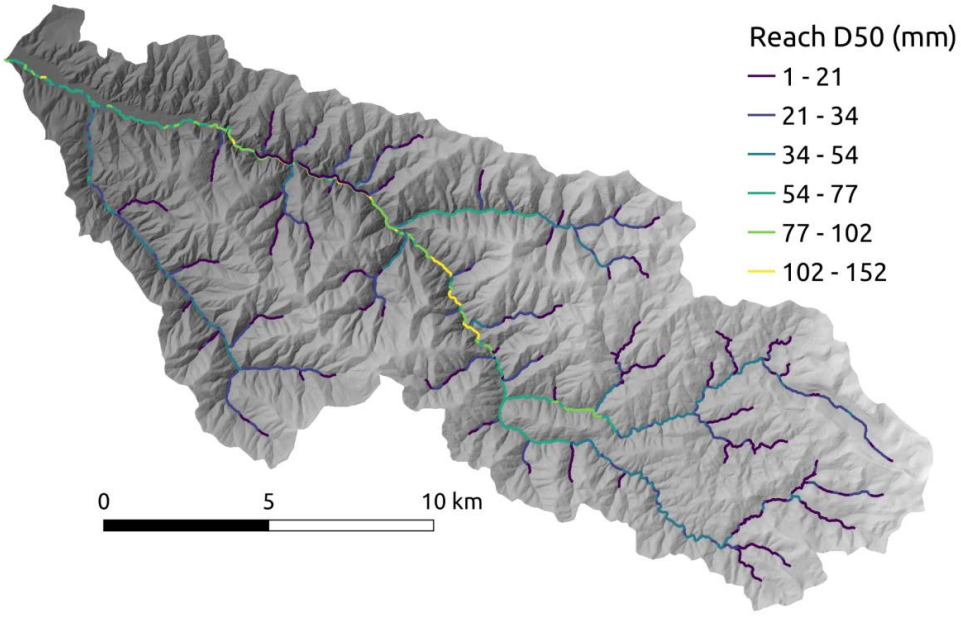

Figure 4. The drainage network for the Sleeping Child Creek basin, with each reach attributed by its predicted D_{50} value. The network is overlain on a hillshade to show the topography hypothesized to result in uniformly high hill-slope channel connectivity.

https://doi.org/10.5194/egusphere-2025-1848
Preprint. Discussion started: 12 June 2025

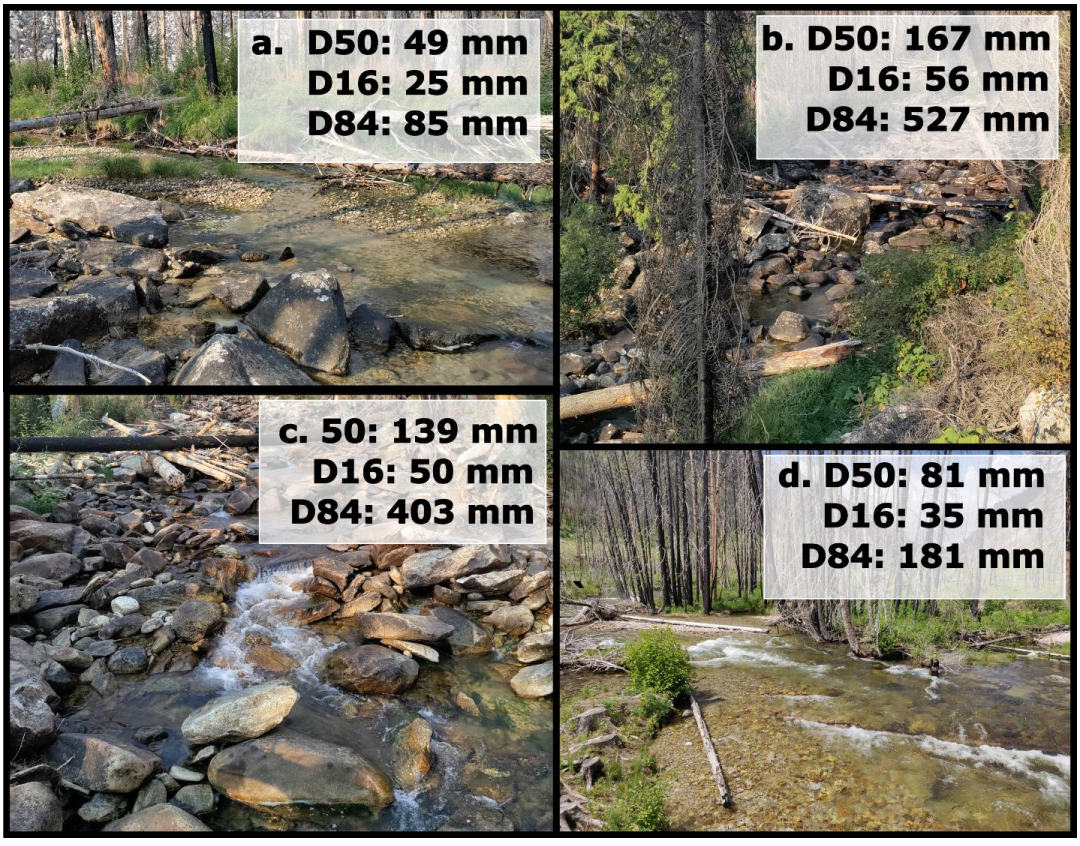

295 **Figure 5. Photographs along different reaches of Roaring Lion Creek with the predicted D_{16}, D_{50}, and D_{84} values.**

The .json format is simply a form of text file that is useful for storing information in a human readable format that is also interoperable with various programming languages. The output .json from the tool stores all of the grain size information produced by the tool for each reach. Specifically, this includes the calculated D_{16}, D_{50}, and D_{84}, as well
300 as the fraction of each half-phi size interval in the full GSD.

https://doi.org/10.5194/egusphere-2025-1848
Preprint. Discussion started: 12 June 2025

5 Discussion and Conclusion

One of the limitations of the tool is that by using variables related to flow competence to predict grain sizes, it assumes that grain size distributions are hydrologically driven. In mountain drainage basins, as previously mentioned, grain sizes can be driven by, and vary greatly as a function of hillslope-channel connectivity and associated erosion and transport processes. As a result, mountain drainage networks often include channels that are completely non-alluvial, whose bed composition is entirely a function of non-fluvial processes (e.g., glacial erosion, rockfall, or other hillslope sediment production processes). In these cases, where the GSD is entirely a function of hillslope sediment delivery with no fluvial reworking, this model is not applicable for predicting grain sizes. In our study basins, the majority of the sediment delivered from hillslopes to channels in the uniform group watersheds is mobile at some flood flows. As a result, our prediction errors were fairly uniform across all sites. In contrast, much of the sediment delivered from hillslopes to channels in the variable group basins is large enough to be immobile at all flows. As a result, prediction errors in these basins were more variable. Overall, results from the application of this algorithm presented here suggest that even in mountainous watersheds where GSDs are also a function of hillslope processes, using a hydraulics-based approach for estimating GSDs provides reasonable estimates.

In this application, I used single pebble counts to represent the GSD of entire reaches in the interest of gathering broad spatial coverage. Reaches are better characterized by performing pebble counts within each distinct geomorphic unit present, and subsequently taking the area-weighted mean (Kondolf, 1997). In applications where higher accuracy is desired for a smaller geographic area, calibrating the model with these types of pebble counts may produce better results.

Comparing measured GSDs to aerial imagery for very coarse-bedded reaches suggests that I may have had a bias for the wetted channel at the time of sampling. Consequently, I may have underestimated the size distribution by oversampling the more mobile fraction present near the thalweg relative to other, coarser grains distributed throughout the channel (Figure 6). In very coarse beds, where it is more challenging to walk over the whole bed, a random walk sampling frame is likely less applicable and less effective. In these cases, a different sampling frame (e.g. gridded sampling) could improve sampling of all sizes present in the bed.

https://doi.org/10.5194/egusphere-2025-1848
Preprint. Discussion started: 12 June 2025

Figure 6. Aerial imagery of a sample reach of Blodgett Creek with a scale bar. The wetted portions of the channel have a finer GSD than the bed as a whole.

Within the uniform group, when using a basin with metamorphic lithology for calibration, errors were the greatest in the one sub-basin underlain by different geology. This highlights the control geology plays on GSDs, and consequently sediment yield, in line with previous findings that geology is a primary control on sediment supply to channels in the Northern Rocky Mountains (Mueller & Pitlick, 2013). While geology exerts control at the landscape scale, other factors can influence variation and GSD at local scales; for example confinement (O'Brien et al., 2019), large wood (Welling et al., 2021; Wohl & Scott, 2017), and beaver dam building activity (Levine & Meyer, 2014). These factors are not included in the model, but should be considered when applying it.

https://doi.org/10.5194/egusphere-2025-1848
Preprint. Discussion started: 12 June 2025

The spatial variability in channel bed grain sizes arises from the interplay between sediment delivery, both from upstream and from adjacent hillslopes, and the competence of the flow to transport that material. These differences can create large variability in transport rates from reach to reach, driving heterogeneity in fluvial sediment connectivity with implications for landscape evolution, habitat, and human infrastructure. The algorithm presented here provides an easily applicable method to use pebble counts to extrapolate estimates for full GSDs to an entire drainage network, allowing for increased accuracy in watershed-scale sediment transport estimates.

Data Availability

The pebble counts used in this work are available at Gilbert (2024b)

Code Availability

grain-size version 1.2.0

Contact: jordan.gilbert@usu.edu

Hardware requirements: PC

Program language: Python

Software required: Minimum processing power required

Program size: 70 KB

The code for applying the algorithm is found at https://github.com/jtgilbert/grain-size (Gilbert 2024c)

Competing Interests

The author declares that he has no conflict of interest.

Acknowledgements

I thank Andrew Wilcox for advising me in the work that this manuscript was a part of and for reviewing this manuscript, and Jean Dixon, Brendan Murphy, Payton Gardner, and Doug Brinkerhoff for their reviews of this work. I thank the Bitterroot National Forest, where field work was conducted.

DGEFinancial Support

This work was supported by the National Science Foundation (NSF DGE 1633831, NSF EAR 1644619).

References

https://doi.org/10.5194/egusphere-2025-1848
Preprint. Discussion started: 12 June 2025

Abeshu, G. W., H. Y. Li, Z. Zhu, Z. Tan, and L. R. Leung. (2022). Median Bed-Material Sediment Particle Size across Rivers in the Contiguous US. *Earth System Science Data 14* (2): 929–42.

Buffington, J. M., Montgomery, D. R., & Greenberg, H. M. (2004). Basin-scale availability of salmonid spawning gravel as influenced by channel type and hydraulic roughness in mountain catchments. *Canadian Journal of Fisheries and Aquatic Sciences. Journal Canadien Des Sciences Halieutiques et Aquatiques*, *61*(11), 2085–2096.

Bunte, K., & Abt, S. R. (2001). Sampling frame for improving pebble count accuracy in coarse gravel-bed streams. *Journal of the American Water Resources Association*, *37*(4), 1001–1014.

Buscombe, D. (2008). Estimation of grain-size distributions and associated parameters from digital images of sediment. *Sedimentary Geology*, *210*(1), 1–10.

Cohen, Sagy, Jaia Syvitski, Thomas Ashley, Roderick Lammers, Balazs Fekete, and Hong-Yi Li. (2022). Spatial Trends and Drivers of Bedload and Suspended Sediment Fluxes in Global Rivers. *Water Resources Research 58* (6): e2021WR031583.

Czuba, J. A. (2018). A Lagrangian framework for exploring complexities of mixed-size sediment transport in gravel-bedded river networks. *Geomorphology , 321*, 146–152.

Gilbert, J. T., & Wilcox, A. C. (2020). Sediment routing and floodplain exchange (SeRFE): A spatially explicit model of sediment balance and connectivity through river networks. *Journal of Advances in Modeling Earth Systems*, *12*(9).

Gilbert, J., & Wilcox, A. C. (2024a). Estimating grain stress and distinguishing between mobility and transportability improves bedload transport estimates in coarse-bedded mountain rivers. Journal of Geophysical Research: Earth Surface, 129(8), e2024JF007662.

Gilbert, J. (2024b). Data for manuscript: An extrapolation algorithm for estimating river bed grain size distributions across basins [Data set]. Zenodo. https://doi.org/10.5281/zenodo.14200058

Gilbert, J. (2024c). jtgilbert/grain-size: Grain Size Distribution Tool (1.2.0). Zenodo. https://doi.org/10.5281/zenodo.14199346

https://doi.org/10.5194/egusphere-2025-1848
Preprint. Discussion started: 12 June 2025

Gorman, A. M., Whiting, P. J., Neeson, T. M., & Koonce, J. F. (2011). Channel substrate prediction from GIS for habitat estimation in Lake Erie tributaries. *Journal of Great Lakes Research*, *37*(4), 725–731.

Hassan, M. A., Bird, S., Reid, D., Ferrer-Boix, C., Hogan, D., Brardinoni, F., & Chartrand, S. (2019). Variable hillslope-channel coupling and channel characteristics of forested mountain streams in glaciated landscapes. *Earth Surface Processes and Landforms*, *44*(3), 736–751.

Ibbeken, H., & Schleyer, R. (1986). Photo-sieving: A method for grain-size analysis of coarse-grained, unconsolidated bedding surfaces. *Earth Surface Processes and Landforms*, *11*(1), 59–77.

Jha, Manoj K., Dawit M. Asamen, Peter M. Allen, Jeffrey G. Arnold, Michael J. White, and Katrin Bieger. (2022). Streambed Median Grain Size (D50) across the Contiguous U.S. *Water 14* (21): 3378.

Kondolf, G. M. (1997). Application of the pebble count notes on purpose, method, and variants. *Journal of the American Water Resources Association*, *33*(1), 79–87.

Leopold, L. B. (1970). An improved method for size distribution of stream bed gravel. *Water Resources Research*, *6*(5), 1357–1366.

Levine, R., & Meyer, G. A. (2014). Beaver dams and channel sediment dynamics on Odell Creek, Centennial Valley, Montana, USA. *Geomorphology , 205*, 51–64.

Meyer-Peter, E., & Müller, R. (1948). Formulas for bed-load transport. *IAHSR 2nd Meeting, Stockholm, Appendix 2*.

Mueller, E. R., & Pitlick, J. (2013). Sediment supply and channel morphology in mountain river systems: 1. Relative importance of lithology, topography, and climate. *Journal of Geophysical Research, [Solid Earth]*.

Mueller, Erich R., M. Elliot Smith, and John Pitlick. (2016). Lithology-Controlled Evolution of Stream Bed Sediment and Basin-Scale Sediment Yields in Adjacent Mountain Watersheds, Idaho, USA: Lithology-Controlled Evolution Of Stream Bed Sediment and Yields. *Earth Surface Processes and Landforms 41* (13): 1869–83.

Morel, M., Booker, D. J., Gob, F., & Lamouroux, N. (2020). Consistent theoretical and empirical predictions of at-a-station hydraulic geometry exponents in stream reaches. Water Resources Research, 56(10), e2020WR027242.

https://doi.org/10.5194/egusphere-2025-1848
Preprint. Discussion started: 12 June 2025

Neely, Alexander B., and Roman A. DiBiase. (2020). Drainage Area, Bedrock Fracture Spacing, and Weathering Controls on Landscape-scale Patterns in Surface Sediment Grain Size. *Journal of Geophysical Research. Earth Surface 125* (10): e2020JF005560.

O'Brien, G. R., Wheaton, J. M., Fryirs, K., Macfarlane, W. W., Brierley, G., Whitehead, K., Gilbert, J., & Volk, C. (2019). Mapping valley bottom confinement at the network scale. *Earth Surface Processes and Landforms*, *esp.4615*.

Parker, G. (1990). Surface-based bedload transport relation for gravel rivers. *Journal of Hydraulic Research*, *28*(4), 417–436.

Purinton, B., & Bookhagen, B. (2019). Introducing PebbleCounts: A grain-sizing tool for photo surveys of dynamic gravel-bed rivers. *Earth Surface Dynamics Discussions*, 1–33.

Schmitt, R. J. P., Bizzi, S., & Castelletti, A. (2016). Tracking multiple sediment cascades at the river network scale identifies controls and emerging patterns of sediment connectivity. *Water Resources Research*, *52*(5), 3941–3965.

Snelder, Ton H., Nicolas Lamouroux, and Hervé Pella. (2011). Empirical Modelling of Large Scale Patterns in River Bed Surface Grain Size. *Geomorphology (Amsterdam, Netherlands) 127* (3–4): 189–97.

Snyder, N. P., Nesheim, A. O., Wilkins, B. C., & Edmonds, D. A. (2013). Predicting grain size in gravel-bedded rivers using digital elevation models: Application to three Maine watersheds. *GSA Bulletin*, *125*(1-2), 148–163.

Strom K. B., Kuhns R. D., & Lucas H. J. (2010). Comparison of Automated Image-Based Grain Sizing to Standard Pebble-Count Methods. *Journal of Hydraulic Engineering*, *136*(8), 461–473.

Verdian, Joseph P., Leonard S. Sklar, Clifford S. Riebe, and Jeffrey R. Moore. (2021). Sediment Size on Talus Slopes Correlates with Fracture Spacing on Bedrock Cliffs: Implications for Predicting Initial Sediment Size Distributions on Hillslopes. *Earth Surface Dynamics 9* (4): 1073–90.

Welling, R. T., Wilcox, A. C., & Dixon, J. L. (2021). Large wood and sediment storage in a mixed bedrock-alluvial stream, western Montana, USA. *Geomorphology* , *384*, 107703.

Wilcock Peter R., & Crowe Joanna C. (2003). Surface-based Transport Model for Mixed-Size Sediment. *Journal of*

https://doi.org/10.5194/egusphere-2025-1848
Preprint. Discussion started: 12 June 2025

Hydraulic Engineering, *129*(2), 120–128.

Wohl, E. E., Anthony, D. J., Madsen, S. W., & Thompson, D. M. (1996). A comparison of surface sampling methods for coarse fluvial sediments. Water Resources Research, 32(10), 3219-3226.

Wohl, E., & Scott, D. N. (2017). Wood and sediment storage and dynamics in river corridors. *Earth Surface Processes and Landforms*, *42*(1), 5–23.

Wolman, M. G. (1954). A method of sampling coarse river-bed material. *Transactions* , *35*(6), 951.